Rapid multi-layer method on solving optimal endo-atmospheric trajectory of launch vehicles[‡]

C. Wei
weichangzhu@hit.edu.cn

Y. Han
han_ye_peng@126.com

J. Pu (iD)
nosay@hit.edu.cn

Y. Li
liyuan@stu.hit.edu.cn

Department of Aerospace Engineering
Harbin Institute of Technology
Harbin 150001
China

P. Huang
huangpanxing2006@126.com
Beijing Institute of Control Engineering
Beijing 100094
China

ABSTRACT

In order to increase the speed, precision and robustness against the engine failure in solving optimal endo-atmospheric ascent trajectory of a launch vehicle, a rapid multi-layer solving method with improved numerical algorithms was proposed. The proposed method is capable of decomposing a large number of intervals into multiple layers with advantageous convergence property. Firstly, the problem of solving optimal endo-atmospheric ascent trajectory, which was subjected to path constraints and terminal constraints, was transformed into a Hamilton Two Point Boundary Value Problem (TPBVP). Then, through the finite difference method and numerical solving algorithm, the Hamilton TPBVP was iteratively solved with fewer initial discrete intervals. The initial values of higher-layer iterations were obtained by interpolating convergent solutions at sparse nodes into the doubly discrete nodes of high

---

[‡] The original published version of this paper was incorrect. A notice detailing this has been published, and the incorrect online PDF and HTML versions have been replaced.

---

layers. The process was repeatedly performed until the solving precision met the requirements. To decrease the calculation load in solving TPBVPs, two improved solving algorithms without and with fewer Jacobian calculations were studied, respectively the Derivative-free Spectral Algorithm for Nonlinear Equations(DF-SANE) combined with the improved derivative-free nonmonotone line search strategy, and the Modified Newton method with a relaxation factor in combination with the Inverse Broyden Quasi-Newton method, denoted as 'MN-IBQ'. Simulation verifications showed that the multi-layer method had significantly higher solving speed than the single-layer method. For the improved numerical algorithms, the DF-SANE was trapped in the local convergence problem. While using the proposed MN-IBQ can further increase the solving rate. Typical engine failure simulations showed that the multi-layer method with the MN-IBQ algorithm had not only significantly higher solving speed but also stronger robustness, where the traditional single-layer method could not adapt. In addition, the thrust loss tolerance limits for the multi-layer solving method were given for different engine failure times. The results show promising potential of the proposed approach in trajectory online generation and closed-loop guidance of launch vehicles at the endo-atmospheric ascent stage.

Keywords: Hamilton two-point boundary value problem; launch vehicle; optimal endo-atmospheric trajectory; multi-layer iteration; inverse Broyden quasi-Newton method

1.0 INTRODUCTION

With the development of advanced launch vehicles, high-precision and high-reliability guidance has become increasingly important and challenging, especially during the endo-atmospheric ascent phase in dense atmosphere. To meet the needs of rapidly developing space in the future, rapid trajectory onboard regeneration and closed-loop guidance are essential to responsive launch, engine failure processing, target orbit change and other major projects. To realise high precision endo-atmospheric guidance of launch vehicles, online solving speed is a crucial factor[1,2]. Therefore, it is necessary to make further studies to improve the solving efficiency of guidance algorithms.

The basic requirement of the endo-atmosphere close-loop guidance algorithm is to accomplish on-board optimisation and generation of trajectory. Methods on solving optimal control problems can mainly be divided into direct and indirect methods[3]. By using a direct method, the optimal trajectory generation problem is transformed into a nonlinear programming problem(NLP)[4], which can be solved by numerical algorithms, such as Hermite interpolation, Gauss Pseudospectral Method[5,6] and so on. However, due to huge computation load, direct methods are still not feasible ways to realise onboard trajectory generation. In recent years, the indirect method has been widely studied for its application in rapid atmospheric ascent trajectory generation[7,8]. By using an indirect method based on the optimal control theory, the rapid optimal trajectory generation problem is transformed into a Hamilton Two Point Boundary Value Problem (TPBVP). Furthermore, TPBVPs can be transformed into finite difference equations (FDE) by the finite difference method, which can be solved using the Newton method with a relaxation factor[9]. The indirect method has been demonstrated to be a promising method to realise ascent trajectory generation of space shuttles, multi-burn launch vehicles[10] and hypersonic air-breathing vehicles[11]. By improving the convergence property through combining the analytical vacuum initial guess technology with

the homotopy technology, the solving rate can be improved[9,12]. In order to achieve a high-precision solution of TPBVPs, a large number of discrete intervals are needed in the finite difference method, which will lead to low solving rate and poor reliability. This means in actualizing real-time online trajectory generation and closed-loop guidance, higher solving efficiency may be obtained at the expense of calculation precision to a certain extent[13,14].

In addition, the numerical methods presented in the literature for solving the FDE are mainly the traditional Newton method with a relaxation factor, which requires multiple numerical calculations for Jacobian. Therefore, it is necessary for the numerical methods to reduce the number of Jacobian calculations. Recently, some improved quasi-Newton methods and gradient-free numerical solution algorithms for nonlinear equations have been studied and shown great application prospects in solving FDE problems.

This paper aims at developing high-efficiency, high-precision and high-robustness algorithms for generation of optimal launch vehicle endo-atmospheric ascent trajectories, especially for engine failure conditions. A rapid multi-layer solving method with improved numerical algorithms is proposed on the basis of traditional solving algorithms. Firstly, the optimal endo-atmospheric ascent problem of a launch vehicle, which is subjected to path constraints and terminal constraints, was transformed into a TPBVP[10]. Subsequently, the finite difference method was used to transform the TPBVP into nonlinear algebraic equations, which can be iteratively solved with fewer initial discrete intervals. Then, the initial values of higher-layer iterations were obtained by interpolating convergent solutions at sparse nodes into doubly discrete nodes of higher layers. The process was repeatedly performed until the solving precision met the requirements. In order to decrease the calculation load in solving the FDE, two improved solving methods without and with fewer Jacobian calculations were studied. For the method without Jacobian calculations, the Derivative-free Spectral Algorithm for Nonlinear Equations combined with the improved derivative-free nonmonotone line search strategy was introduced. For the method with fewer Jacobian calculations, the MN-IBQ algorithm was applied. The iteration number in the proposed multi-layer solving method requires fewer iterations compared with traditional algorithms, which leads to improved speed in solving optimal endo-atmospheric ascent trajectory. Simulation verifications showed that the proposed multi-layer solving method had a significant advantage over the traditional solving method in terms of calculation rate. The proposed multi-layer method with the MN-IBQ algorithm had not only significantly higher solving speed but also stronger robustness against the engine failure, where the traditional single-layer method cannot adapt.

2.0 OPTIMAL ENDO-ATMOSPHERIC ASCENT MODEL OF LAUNCH VEHICLES

2.1 Endo-atmospheric motion mathematical model

To increase stability and accuracy of the numerical calculation, a non-dimensional motion mathematical model was adopted. Non-dimensional motion equations of a launch vehicle in the Launch Inertial Coordinate System are as follows[13]:

$$
\begin{aligned}
\dot{\boldsymbol{r}} &= \boldsymbol{V} \\
\dot{\boldsymbol{V}} &= -\boldsymbol{r}/r^3 + (T-A)\boldsymbol{I}_b + N\boldsymbol{I}_n
\end{aligned}
\qquad \dots (1)
$$

where $\boldsymbol{r}$ and $\boldsymbol{V} \in R^3$ are the geocentric distance vector and velocity vector, respectively; T represents the non-dimensional engine thrust acceleration; A and N represent the non-dimensional aerodynamic acceleration in axial and normal directions, respectively; $\boldsymbol{I}_b$ is the unit vector in the axial direction of the launch vehicle; $\boldsymbol{I}_n$ is the unit vector perpendicular to $\boldsymbol{I}_b$ located within the longitudinal symmetry plane of the launch vehicle.

In order to ensure structure safety, the endo-atmospheric ascent flight of the launch vehicle needs to satisfy some path constraints. The aerodynamic bending moment constraint (product of attack angle and dynamic pressure) was taken into consideration in this study

$$S = |q\alpha| - Q_\alpha \leq 0 \qquad \ldots (2)$$

where $q = \rho V_r^2 / 2$; Q_α is the allowable maximum aerodynamic bending moment.

Normally terminal constraints are considered as standard burnout conditions, including geocentric distance r_f^*, velocity V_f^*, orbit inclination i^* and flight path angle γ_f^*, which are equivalent to the given semi-major axis, eccentricity, orbit inclination and true anomaly at burnout time. Terminal constraints are represented as:

$$
\begin{aligned}
&\frac{1}{2}\boldsymbol{r}_f^T \boldsymbol{r}_f - \frac{1}{2}r_f^{*2} = 0 \\
&\boldsymbol{I}_N^T(\boldsymbol{r}_f \times \boldsymbol{V}_f) - \|\boldsymbol{r}_f \times \boldsymbol{V}_f\| \cos i^* = 0 \\
&\boldsymbol{r}_f^T \boldsymbol{V}_f - r_f V_f \sin \gamma_f^* = 0 \\
&\frac{1}{2}\boldsymbol{V}_f^T \boldsymbol{V}_f - \frac{1}{2}V_f^{*2} = 0
\end{aligned}
\qquad \ldots (3)
$$

Then, the optimal endo-atmospheric ascent problem can be equivalent to finding the optimal body-axis direction $\boldsymbol{I}_b$ and engine burnout time t_f according to the current initial conditions, so as to make the trajectory of the launch vehicle reach the given final conditions at burnout time with the path constraints being satisfied.

2.2 Optimal control model

Generally, a double-layer iterative method is adopted to solve the optimal endo-atmospheric ascent problem of a launch vehicle[13]. For the internal layer, an optimal control algorithm is adopted to solve the ascent trajectory problem of acquired maximum terminal energy at given flight time; whereas for the external layer, the secant method is employed to iteratively solve the flight time to meet the terminal velocity constraint. A rapid, accurate and reliable solution of optimal ascent trajectory at the internal layer is the key to realising rapid optimal trajectory generation, as well as the research focus of this paper.

Performance index is selected as:

$$J = \phi(\boldsymbol{r}_f, \boldsymbol{V}_f, t_f) = 1/r_f - V_f^2 \qquad \ldots (4)$$

In the application of the optimal control theory, the Hamiltonian function considering the path constraints is represented as:

$$H = \boldsymbol{p}_r^T \boldsymbol{V} + \boldsymbol{p}_V^T \left[-\boldsymbol{r}/r^3 + (T - A)\boldsymbol{I}_b + N\boldsymbol{I}_n \right] + \lambda_{q\alpha} S \qquad \ldots (5)$$

where p_r and $p_V \in R^3$ are co-state variables; $\lambda_{q\alpha}$ is the scalar multiplier; when $S < 0, \lambda_{q\alpha} = 0$ and when $S = 0, \lambda_{q\alpha} = (\partial H / \partial \alpha)/q$.

According to the standard first order necessary conditions for the optimal solution, differential equations of co-state variables involve the calculation of partial derivatives of vectors, and the forms are relatively complex. According to control equations, the optimal body-axis expression can be derived as[13]:

$$\mathbf{1}_b^* = \left(\frac{\sin \alpha}{\sin \Phi} \right) \mathbf{1}_{p_V} + \left[\frac{\cos \alpha - \cos \Phi \cos(\Phi - \alpha)}{\sin^2 \Phi} \right] \mathbf{1}_{V_r} \qquad \dots (6)$$

where Φ is the angle between p_V and V_r; $\mathbf{1}_{p_V}$ is the unit vector of p_V; α is obtained by solving $\tan(\Phi - \alpha)(T - A + N_\alpha) - (A_\alpha + N) = 0$.

According to the transversal conditions, three terminal constraint conditions are obtained:

$$(V_f^T p_{r_f}) r_f^2 - (r_f^T p_{V_f}) V_f^2 + (r_f^T V_f)(V_f^2 - r_f^T p_{r_f}) = 0$$
$$V_f^T p_{V_f} - V_f^2 = 0 \qquad \dots (7)$$
$$(H_f^T p_{r_f}) \left[H_f^T (r_f \times \mathbf{1}_N) + (H_f^T p_{V_f})(H_f^T (V_f \times \mathbf{1}_N)) \right] = 0$$

where, $H_f = r_f \times V_f$.

Equation (7) and the first three constraints in Equation (3) constitute six terminal boundary conditions.

Based on the above derivation, the optimal ascent problem of a launch vehicle can be converted into a TPBVP consisting of differential equations of state variables and co-state variables, initial state conditions and terminal boundary conditions. By giving definitions of $x = (r^T, V^T)^T, p = (p_r^T, p_V^T)^T$, and $y = (x^T, p^T)^T \in R^{12}$, the model can be expressed as

$$\dot{y} = f(t, y)$$
$$B_0(y_0) = 0 \qquad \dots (8)$$
$$B_f(y_f) = 0$$

where B_0 is the given six initial state conditions $x(t_0)$; B_f is the six terminal boundary conditions. The TPBVP can be depicted as: to find initial values $p(t_0)$ of co-state variables that make the system $\dot{y} = f(t, y)$ meet boundary conditions $B_f = 0$ at the terminal.

3.0 RAPID MULTI-LAYER SOLVING METHOD

The model of the TPBVP provided in Equation (8) is very complex. The finite difference method is one of the classical solving methods currently used[9], which discretizes nonlinear differential equations into linear algebraic equations through central finite difference. The principle of the method is as follows:

The time interval $t_f - t_0$ is divided into M subintervals with an identical length of $h = (t_f - t_0)/M$. Then differential equations in Equation (8) can be obtained by central finite difference approximation:

$$\frac{1}{h}(y_k - y_{k-1}) = f\left(t_{k-1/2}, \frac{y_k + y_{k-1}}{2} \right) \qquad \dots (9)$$

The above equations can be rewritten as the finite difference equations (FDE) as follows

$$E_k(\boldsymbol{y}_k, \boldsymbol{y}_{k-1}) = \boldsymbol{y}_k - \boldsymbol{y}_{k-1} - hf\left(t_{k-1/2}, \frac{\boldsymbol{y}_k + \boldsymbol{y}_{k-1}}{2}\right) = 0 \qquad \dots (10)$$

where $\boldsymbol{E}_0 = [\boldsymbol{B}_0^{\mathrm{T}}, \boldsymbol{B}_f^{\mathrm{T}}]^{\mathrm{T}}$, and the TPBVP is then converted into a problem of solving $\boldsymbol{Y} = (\boldsymbol{y}_0^{\mathrm{T}}, \boldsymbol{y}_1^{\mathrm{T}} \dots \boldsymbol{y}_M^{\mathrm{T}})^{\mathrm{T}} \in R^{12(M+1)}$, the solution of $12(M+1)$ nonlinear algebraic equations $\boldsymbol{E} = (\boldsymbol{E}_0^{\mathrm{T}}, \boldsymbol{E}_1^{\mathrm{T}} \dots \boldsymbol{E}_M^{\mathrm{T}})^{\mathrm{T}}$.

When the finite difference method is used to solve optimal ascent trajectory of a launch vehicle, attention should be paid to the following points:

1) A homotopy technique is needed (taking the atmospheric density or reference area as homotopy parameters) to ensure reliable convergence of the algorithm. The required homotopy time increases with the number of discrete intervals increasing;

2) More discrete intervals, unknown node variables and density homotopy times are needed to obtain higher solving precision, which greatly reduces the solving efficiency of the algorithm;

3) Fewer discrete intervals and unknown node variables are needed to improve solving efficiency, so as to ensure real-time performance of trajectory online generation and closed-loop guidance. However, this will cause the loss of solving precision, making it impossible to realise optimal closed-loop guidance in a real sense.

In order to remedy the weakness, this paper puts forward a rapid multi-layer solving method. First, the problem was solved with fewer initial discrete intervals; then, the interpolation values, which were obtained by interpolating convergent solutions at sparse nodes into doubly discrete nodes of higher layers, were taken as initial values to carry out higher-layer iterations. The process was repeatedly performed until the solving precision met requirements. The implementation steps are as follows:

(1) The initial value of the higher-layer iteration is obtained by solving the TPBVP based on fewer initial discrete intervals:

  i. The initial values of engine burnout time and layer number K are set to t_{f_0} and 0, respectively; the number of discrete intervals is set as $M = N_0$, wherein N_0 depends on the engine burnout time and is set to be smaller than 10.

  ii. The analytic vacuum solution of the non-constraint optimal ascent problem is taken as the iterative initial value $\boldsymbol{Y}_0$;

  iii. By the finite difference method, the optimal ascent trajectory problem of acquired maximum terminal energy with fixed final time is transformed into FDE, which is iteratively solved by a numerical algorithm, such as the traditional Newton method with a relaxation factor.

For the lower-layer iteration, the homotopy technology is necessary to obtain a full atmospheric solution, whose continuation form is only the reference area;

$$\hat{S} = \varepsilon S, 0 \leq \varepsilon \leq 1 \qquad \dots (11)$$

The homotopic parameter ε is initially set to 0 for the vacuum solution and gradually increases to unity for the full atmospheric solution, that is, $\varepsilon = 1$. The convergent solution for the current value of ε serves as the starting point of the solution for the next value of ε till $\varepsilon = 1$.
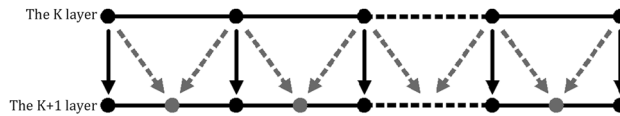
Figure 1. Diagram of multi-layer recursion.

iv. Engine burnout time t_f is adjusted by the secant method to meet the terminal velocity constraint. State variables, co-state variables and t_f at fewer discrete interval nodes are obtained.

(2) The TPBVP is solved with the multi-layer iteration method:

i. End if the desirable solving precision is obtained, otherwise double the time grid density, $K = K + 1$;

ii. State variables and co-state variables at layer K obtained in step 1) are allocated to newly increased nodes at layer $K + 1$ through Lagrange interpolation, as shown in Fig. 1;

iii. The state variables, co-state variables and t_f at nodes at layer $K + 1$ are obtained by using the method of iii and iv in step 1), wherein the homotopy technology is not applied;

iv. Return to step i.

3.1 Improved numerical solution for finite difference equation

By introducing a multi-layer solving strategy, the solving efficiency and adaptability have been improved. Moreover, two improved numerical algorithms without and with fewer Jacobian calculations are proposed for solving the finite difference equation, in order to further improve the solving efficiency from the aspect of the numerical algorithm.

The Newton iteration method with a relaxation factor is usually used to solve the FDE through combined applications of the analytical vacuum initial guess technology and homotopy technology[13]. The update of Y is given by:

$$
\begin{aligned}
Y_j &= Y_{j-1} + \sigma_j d_j \ \ 0 < \sigma_j \le 1 \\
d_j &= - \left[\frac{\partial E(Y_{j-1})}{\partial Y} \right]^{-1} E(Y_{j-1})
\end{aligned}
\qquad \dots (12)
$$

where, the relaxation factor σ_j is determined by the following monotone criterion:

$$
\sigma_j = \max_{0 \le i} \left\{ \beta^i | E^T \left[Y_{j-1} + \beta^i d_j \right] E \left[Y_{j-1} + \beta^i d_j \right] < E^T (Y_{j-1}) E(Y_{j-1}) \right\}, \ 0 < \beta < 1 \qquad \dots (13)
$$

A significant disadvantage of the Newton iterative method is that the Jacobian must be calculated in each iteration, which accounts for a large proportion of numerical computation load. Therefore, improved solving methods without or with fewer Jacobian calculations should be studied.

Traditional solving algorithms require gradient calculations, such as conjugate gradient methods, spectral gradient methods, and their deformations. Therefore, the key to the derivative-free algorithm is to approximate the gradient with a gradient-free search direction. Motivated by the idea, for solving the nonlinear equations $F(x) = 0$, La Cruz and Raydan[15] introduced a derivative-free algorithm named the Derivative-free Spectral Algorithm for Nonlinear Equations (DF-SANE). This algorithm extends the spectral gradient approach and uses the residual $d_k = \pm F(x_j)$ as search directions. Moreover, a merit function

$f(x) = \frac{1}{2}[\boldsymbol{F}(x)]^2$ with the property that $f(x) = 0 \Leftrightarrow \boldsymbol{F}(x) = 0$ is introduced. The first trial point at each iteration is $\boldsymbol{Y}_j = \boldsymbol{Y}_{j-1} + \sigma_j \boldsymbol{E}(\boldsymbol{Y}_{j-1})$ where σ_j is a spectral coefficient.

$$\sigma_j = \frac{s'_{j-1}s_{j-1}}{s'_{j-1}y_{j-1}}$$
$$s_{j-1} = \boldsymbol{Y}_j - \boldsymbol{Y}_{j-1}, y_{j-1} = \boldsymbol{E}(\boldsymbol{Y}_j) - \boldsymbol{E}(\boldsymbol{Y}_{j-1}) \qquad \dots (14)$$

The spectral coefficient σ_j is an appropriate Rayleigh quotient with respect to a secant approximation of the Jacobian.

$$\frac{\left\langle \left[\int_0^1 \boldsymbol{J}(x_j + ts_j)\,\mathrm{d}t\right] s_j, s_j \right\rangle}{\langle s_j, s_j \rangle} \qquad \dots (15)$$

which makes it attractive for the numerical solution of (10).

Since $\boldsymbol{d}_k = \pm \boldsymbol{F}(x_k)$ is not necessarily a descent direction, the global convergence is guaranteed by an effective line search strategy. The majority of line search methods require a decrease in the objective function $f(x)$ at each iteration, which means that the corresponding sequence of function values monotonically decreases. This may result in a slow convergence. On the other hand, the nonmonotone line search strategies could converge faster and avoid the local convergence problem.

The well-known nonmonotone line-search technique was introduced by Grippo, Lampariello and Lucidi(GLL)[16]. Li and Fukushima[17] presented the LF method that avoided the necessity of descent directions to guarantee that each iteration was well defined.

The GLL condition can be written as follows:

$$f(x_k + \alpha_k d_k) \leq \bar{f}_k + \gamma \alpha_k \nabla f(x_k)^T d_k, \bar{f}_k = \max_{0 \leq j < M-1} f(x_{k-j}) \qquad \dots (16)$$

The LF condition can be written as follows:

$$\|F(x_k + \alpha_k d_k)\| \leq (1 + \eta_k) \|F(x_k)\| - \gamma \alpha_k^2 \|d_k\|_2^2 \qquad \dots (17)$$

The GLL strategy tolerates an increase in the objective function (nonmonotonic behavior), but requires the gradient and descent directions to guarantee global convergence. The LF strategy accepts nondescent directions but the nonmonotone behavior is insufficient.

By taking into account the advantages of both schemes, the new nonmonotone line search condition for DF-SANE can be written as:

$$f(x_{k+1}) \leq \bar{f}_k + \eta_k - \gamma \alpha_k^2 f(x_k), \bar{f}_k = \max_{0 \leq j < M-1} f(x_{k-j}) \qquad \dots (18)$$

The GLL term $\max_{0 \leq j < M-1} f(x_{k-j})$ guarantees the sufficient nonmonotonicity of $f(x_k)$; η_k is responsible for the result that all the iterations are well defined; and the term $-\gamma \alpha_k^2 f(x_k)$ is responsible for improving the global convergence property.

Step 0. Set $k = 0$.

Step 1. Choose σ_k such that $|\sigma_k| \in [\sigma_{\min}, \sigma_{\max}]$ (the spectral coefficient)

$$\bar{f}_k = \max\left\{f(x_k), \cdots, f(x_{\max\{0,k-M+1\}})\right\}$$

Set $d = -\sigma_k F(x_k), \alpha_+ = 1, \alpha_- = -1$

Step 2. If $f(x_k + \alpha_+ d) \leq \bar{f}_k + \eta_k - \gamma \alpha_+^2 f(x_k)$ then define $d_k = d, \alpha_k = \alpha_+, x_{k+1} = x_k + \alpha_k d_k$

Else if $f(x_k - \alpha_- d) \leq \bar{f}_k + \eta_k - \gamma \alpha_-^2 f(x_k)$ then define $d_k = -d, \alpha_k = \alpha_-, x_{k+1} = x_k + \alpha_k d_k$

Else Choose $\alpha_{+new} \in [\tau_{\min}\alpha_+, \tau_{\max}\alpha_+], \alpha_{-new} \in [\tau_{\min}\alpha_-, \tau_{\max}\alpha_-]$.

$$\alpha_{+new} = \begin{cases} \tau_{\min}\alpha_+ & \text{if } \alpha_t < \tau_{\min}\alpha_+ \\ \tau_{\max}\alpha_+ & \text{if } \alpha_t > \tau_{\max}\alpha_+ \\ \alpha_t & \text{otherwise} \end{cases} \qquad \ldots (19)$$

where

$$\alpha_t = \frac{\alpha_+^2 f(x_k)}{f(x_k + \alpha_+ d) + (2\alpha_+ - 1)f(x_k)}$$

Replace $\alpha_{+new} = \alpha_+, \alpha_{-new} = \alpha_-$ and go to Step 2.

Step 3. If $\|F(x_{k+1})\| < \varepsilon$, terminate the execution of the algorithm. Else, $k = k + 1$ and go to Step 1.

However, since the search direction is not the descent direction, the DF-SANE method may be trapped in local convergence problems. Therefore, an improved solving algorithm with fewer Jacobian calculations is also proposed in this paper. In order to reduce the calculation load of solving the FDE in Equation (10), a modified Newton method with a relaxation factor in combination with the inverse Broyden quasi-Newton method is applied, denoted as "MN-IBQ". Through combining the advantages of the Newton method and the simple Newton method, the modified Newton method is capable of performing the Jacobian calculation once every two steps, which not only preserves the fast convergence property of the Newton method, but also reduces the number of Jacobian calculations. The formula for the modified Newton method with a relaxation factor is as follows:

The search direction $\boldsymbol{d}_j$ in the j-th iteration is determined by solving the linear algebraic equations

$$\begin{aligned} \boldsymbol{Y}_{j-1,0} &= \boldsymbol{Y}_{j-1} \\ \boldsymbol{Y}_{j-1,1} &= \boldsymbol{Y}_{j-1} - \sigma_{j,1} \left[\frac{\partial \boldsymbol{E}(\boldsymbol{Y}_{j-1})}{\partial \boldsymbol{Y}} \right]^{-1} \boldsymbol{E}(\boldsymbol{Y}_{j-1}) \ j = 1, 2, \cdots \qquad \ldots (20) \\ \boldsymbol{Y}_j &= \boldsymbol{Y}_{j-1,1} - \sigma_{j,2} \left[\frac{\partial \boldsymbol{E}(\boldsymbol{Y}_{j-1})}{\partial \boldsymbol{Y}} \right]^{-1} \boldsymbol{E}(\boldsymbol{Y}_{j-1,1}) \end{aligned}$$

Such search step size ensures that the sequence $\{\|\boldsymbol{E}(\boldsymbol{Y}_{j-1})\|\}$ is monotonically decreasing. Convergence is achieved when $\|\boldsymbol{E}(\boldsymbol{Y}_{j-1})\|$ is not greater than a preselected tolerance.

Next, the step size parameters $\sigma_{j,1}, \sigma_{j,2}$ are determined by the following criterion:

$$\sigma_{j,1} = \max_{0 \leq i} \left\{ \beta^i | \boldsymbol{E}^{\mathrm{T}} \left[\boldsymbol{Y}_{j-1} + \beta^i \boldsymbol{d}_{j,1} \right] \boldsymbol{E} \left[\boldsymbol{Y}_{j-1} + \beta^i \boldsymbol{d}_{j,1} \right] < \boldsymbol{E}^{\mathrm{T}}(\boldsymbol{Y}_{j-1})\boldsymbol{E}^{\mathrm{T}}(\boldsymbol{Y}_{j-1}) \right\}, 0 < \beta < 1$$

$$\sigma_{j,2} = \max_{0 \leq i} \left\{ \beta^i | \boldsymbol{E}^{\mathrm{T}} \left[\boldsymbol{Y}_{j-1,1} + \beta^i \boldsymbol{d}_{j,2} \right] \boldsymbol{E} \left[\boldsymbol{Y}_{j-1,1} + \beta^i \boldsymbol{d}_{j,2} \right] < \boldsymbol{E}^{\mathrm{T}}(\boldsymbol{Y}_{j-1,1})\boldsymbol{E}^{\mathrm{T}}(\boldsymbol{Y}_{j-1,1}) \right\}, 0 < \beta < 1$$

$$\boldsymbol{d}_{j,1} = \left[\frac{\partial \boldsymbol{E}(\boldsymbol{Y}_{j-1})}{\partial \boldsymbol{Y}} \right]^{-1} \boldsymbol{E}(\boldsymbol{Y}_{j-1}), \boldsymbol{d}_{j,2} = \left[\frac{\partial \boldsymbol{E}(\boldsymbol{Y}_{j-1})}{\partial \boldsymbol{Y}} \right]^{-1} \boldsymbol{E}(\boldsymbol{Y}_{j-1,1}) \qquad \ldots (21)$$

To further improve the solving efficiency, the inverse Broyden quasi-Newton method[18] that requires less computation load is introduced.

The inverse Broyden quasi-Newton method can provide a superlinear convergence rate. Meanwhile, it does not require the Jacobi matrix recalculation or matrix inversion operation, but only needs to determine the H-correction matrix. The iterative formula of the inverse Broyden quasi-Newton method is as follows:

$$
\begin{aligned}
Y_j &= Y_{j-1} - H_{j-1} E(Y_{j-1}) \\
H_j &= H_{j-1} + \Delta H_{j-1} \\
\Delta H_{j-1} &= (r_j - H_{j-1} y_j) \frac{(r_j) H_{j-1}}{(r_j) H_{j-1} y_j}
\end{aligned}
\qquad \ldots (22)
$$

where, $r_j = Y_j - Y_{j-1}, y_j = E(Y_j) - E(Y_{j-1})$.

When applying Equation (22), we need good initial values and H matrix approximations in order to obtain better solutions quickly. Therefore, a hybrid solution can be used, in which the modified Newton iteration method with a relaxation factor is applied firstly until the iteration bias converges to a certain accuracy, and then the inverse Broyden quasi-Newton method is used until the final convergence accuracy is satisfied.

4.0 SIMULATION RESULTS AND DISCUSSION

Simulation verifications were carried out based on a suborbital reusable launch vehicle. The launch vehicle vertically rose for 5.0s after being launched from the ground, and then turned with exponential attack angle for 25.0s. An optimal regeneration of the ascent trajectory after 30.0s was needed to correct the bias caused by the wind disturbance, thrust deviation and aerodynamic parameter deviation. The aerodynamic bending moment was set to be ≤ 0.7 kPa•rad, and the required terminal constraints included a height of 60.0km, a velocity of 2700.0m/s, a flight path angle of 25.3° and an orbit inclination of 15.0°. All the algorithms involved were coded in C and executed in an industrial PC with a 1.0 GHz processor.

Firstly, in order to demonstrate the effectiveness of the multi-layer solving strategy, the multi-layer method was compared with the traditional single-layer method by using the traditional numerical solving algorithm. Secondly, on the basis of the multi-layer solving strategy, to validate the effectiveness of the improved numerical solving algorithm, two improved numerical algorithms were further compared with the traditional one. Thirdly, in order to verify the adaptability of the proposed multi-layer algorithm to thrust loss, the maximum fault degrees corresponding to different fault times were given. Finally, for a typical maximum thrust loss condition, a comparison simulation between the single-layer algorithm and the multi-layer method with improved numerical algorithms was conducted.

To investigate the advantages of the multi-layer solving method proposed over the traditional single-layer direct solving method, a comparison study was carried out for the nominal ascent guidance with different interval numbers $N = 10, 20, 40$. The initial number of discrete intervals N_0 was set to 5. For the two solving methods, the FDE was both solved by the traditional Newton method with a relaxation factor.

According to the optimal guidance command (burnout time and attitude angle) acquired online, the integral state variables of each solving method can be firstly obtained by integrating the dynamic equations in Equation (1), then the solving precision can be checked in terms of deviation between the integral state variables and optimised state variables. Table 1 shows the statistics of the homotopy times, positional accuracy, velocity accuracy and consuming time of CPU of each method.

Table 1
Comparison of simulation results between multi-layer solving method and direct solving method under normal conditions

Interval number	Method	Homotopy times	Position accuracy(m)	Velocity accuracy(m/s)	Time(s)
10	direct solving	3	114.347	0.4138	0.58
10	multi-layer solving ($N=2$)-Traditional	2	114.347	0.4138	0.33
20	direct solving	4	27.8510	0.2461	2.01
20	multi-layer solving ($N=3$)-Traditional	2	27.8510	0.2461	0.82
40	direct solving	6	13.1460	0.0933	9.57
40	multi-layer solving ($N=4$)-Traditional	2	13.1460	0.0933	2.62

From Table 1, the following conclusions can be drawn.

(1) When the number of discrete intervals is the same, the multi-layer solution and traditional direction solution have consistent positional accuracy and velocity accuracy, while the solving efficiency of the multi-layer method is more than 3 times as high as that of the traditional direct solution.
(2) With the increase of the number of discrete intervals, the positional accuracy and velocity accuracy of optimal ascent trajectory gradually increase, and the homotopy time of the direct solution increases gradually, while that of the multi-layer solution remains unchanged.
(3) With the increase of the number of discrete intervals, the consuming time of CPU for the multi-layer solution increases gradually, while the consuming time of CPU for the direct solution increases rapidly.

The multi-layer solving method proposed in this paper has substantial improvements compared with the traditional one. The bigger the number of discrete intervals is, the higher the improved efficiency is. Figures 2–3 respectively show the height and velocity deviation curves when N is set to different values. Both height and velocity deviations reach the maximum at the terminal time. Figures 4–5 respectively show the angle of attack and pitch angle curves calculated by the multi-layer solving method.

On the basis of the multi-layer solving strategy, to validate the effectiveness of the improved numerical algorithm for solving FDE, a comparative analysis of two numerical solutions is conducted, namely the traditional Newton method with a relaxation factor, and the DF-SANE, which are denoted as "-Traditional" and "-DF-SANE", respectively. DF-SANE was implemented with the following parameters: $\sigma_{min} = 1e-10$, $\sigma_{max} = 1e10$, $\tau_{min} = 0.05$, $\tau_{max} = 0.5$, $\eta_k = \|F(x_0)\| / (1+k)^2$, $\gamma = 1e3$, $M = 20$, $\varepsilon = 1e-6$.

The simulation results show that DF-SANE converged to the local minimum and failed to converge to the given ε. The residual curve and search step curve are as follows.

It can be seen from Fig. 6 that the residuals of the equations show obvious nonmonotonicity. The residuals gradually converge from 0.0014 on the overall trend. However, after converging to the local minimum 2.4e-4, the residuals remain stable instead of decreasing, thus failing to converge to the given ε. As can be seen from Fig. 7, after the number of iterations is greater
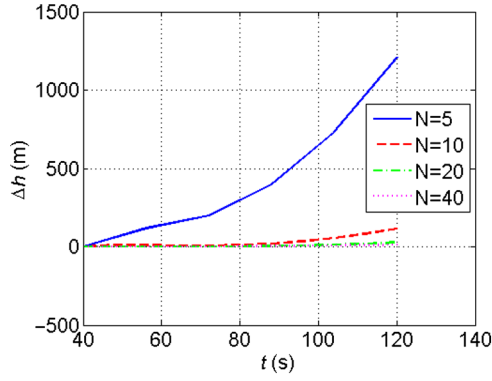
Figure 2. Time-dependent variation of height deviation for normal condition.
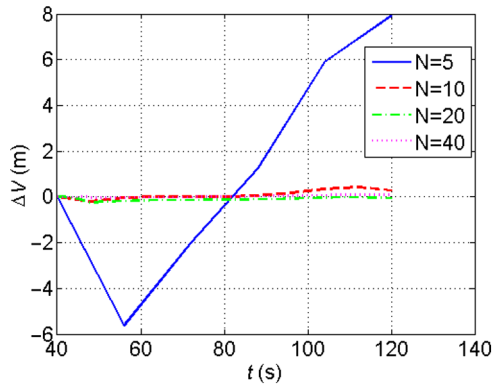

Figure 3. Time-dependent variation of velocity deviation for normal condition.
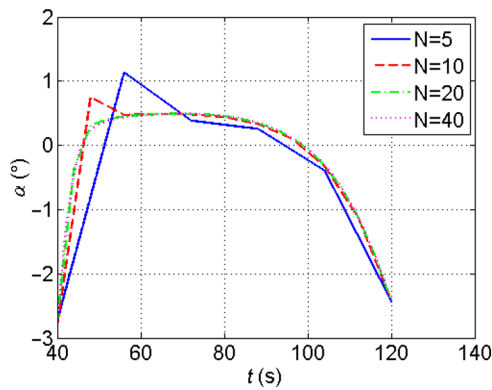

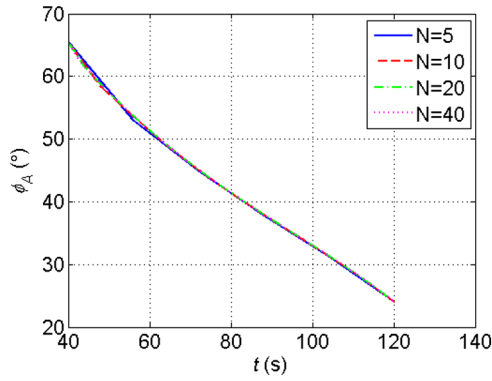Figure 4. Time-dependent variation of angle-of-attack for normal condition.

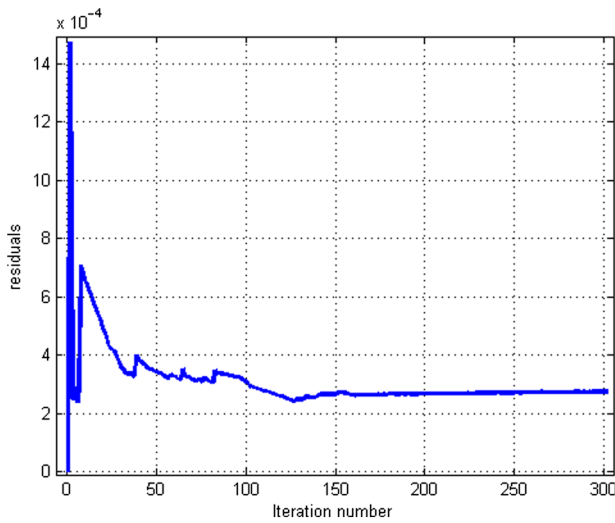Figure 5. Time-dependent variation of pitch angle for normal condition.

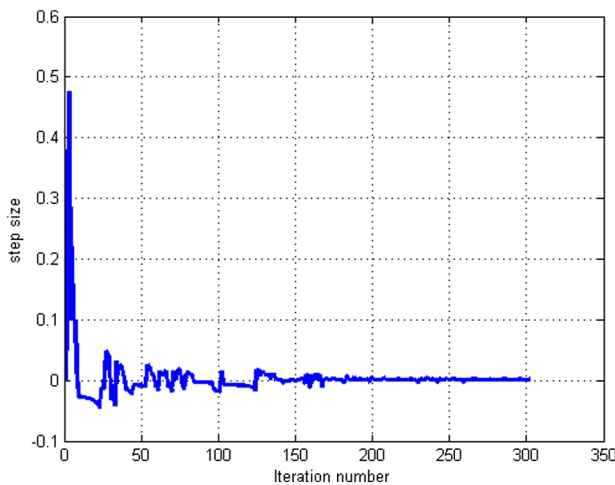Figure 6. Iteration number-dependent variation of residual for normal condition.

Figure 7. Iteration number-dependent variation of step size for normal condition.

Table 2
Comparison of simulation results between traditional and MN-IBQ numerical algorithms for multi-layer solving method under normal conditions

Interval number	Method	Homotopy times	Position accuracy(m)	Velocity accuracy(m/s)	Time(s)
10	($N = 2$)-Traditional	2	114.347	0.4138	0.33
10	($N = 2$)- MN-IBQ	2	114.347	0.4138	0.28
20	($N = 3$)-Traditional	2	27.8510	0.2461	0.82
20	($N = 3$)- MN-IBQ	2	27.8510	0.2461	0.70
40	($N = 4$)-Traditional	2	13.1460	0.0933	2.62
40	($N = 4$)- MN-IBQ	2	13.1460	0.0933	2.20

than 160, the search step size is already less than 0.005. It would seem that the failure of DF-SANE is essentially due to the fact that the search direction in DF-SANE is not the descent direction and the non-monotone linear search method has insufficient global convergence.

Since the DF-SANE method without Jacobian calculations is trapped in the local convergence problem, the improved solving algorithm with fewer Jacobian calculations is proposed in this paper. It is the combination of the modified Newton method with a relaxation factor and the inverse Broyden quasi-Newton method, and denoted as "- MN-IBQ". Meanwhile, the traditional Newton method with a relaxation factor is denoted as "-Traditional". A comparison between MN-IBQ and Traditional is conducted. Table 2 shows the statistics of the homotopy time, positional accuracy, velocity accuracy and consuming time of CPU of each method.

According to Table 2, the following conclusions can be drawn. Through the combination of the modified Newton method with a relaxation factor and the inverse Broyden quasi-Newton method, the solving rate can be increased by approximately 15 percent compared with the traditional Newton method with a relaxation factor.

To verify the adaptability of the proposed multi-layer solving method to thrust loss, a series of case studies with different engine failure times and degrees were carried out. Assuming that the engine fails at different times, the guidance system will perform an optimal trajectory replanning immediately after the failure is detected. The number of the discrete intervals N_0 was set to 40. The accuracy requirements included the position deviation $\Delta r \leq 20m$ and the velocity deviation $\Delta v \leq 0.5m/s$. The results of the maximum thrust loss that the multi-layer solving method could tolerate were given, where the convergent solution would not be obtained in the homotopy process if the thrust loss was a little bigger. Corresponding deviations are shown in the following table.

From Table 3, the following conclusions can be drawn.

1) The earlier the engine failure occurs, the smaller the maximum allowable thrust loss is;
2) The allowable maximum thrust loss increases approximately linearly with the engine failure time.

This experiment analyzed a typical worse situation in which a serious engine failure happened 70 seconds after the vehicle was launched and led to a 25% reduction in thrust. Table 4 shows the statistics of the homotopy time, positional accuracy, velocity accuracy and consuming time of CPU of each method for the case of 25% thrust reduction.

Figures 8–9 respectively show height and velocity deviation curves when N is set to different values. Both height and velocity deviations reach the maximum at the terminal time.

Table 3
**Results of multi-layer solving method under maximum allowable thrust
deviations for different failure time**

Failure time(s)	Maximum thrust loss(%)	Height deviation(m)	Velocity deviation(m/s)
60	17	19.29	0.38
70	25	19.64	0.33
80	32	19.47	0.28
90	38	19.29	0.33
100	45	19.36	0.29
110	51	19.35	0.31

Table 4
**Comparison between multi-layer solving method and direct solving method
under engine failure conditions**

Interval number	Method	Homotopy time	Position accuracy(m)	Velocity accuracy(m/s)	Time(s)
10	direct solving	3	79.00	3.27	0.61
10	multi-layer solving ($N = 2$)-Traditional	2	79.00	3.27	0.36
10	multi-layer solving ($N = 2$)- MN-IBQ	2	79.00	3.27	0.30
20	direct solving	/	/	/	/
20	multi-layer solving ($N = 3$)-Traditional	2	28.09	0.92	0.86
20	multi-layer solving ($N = 3$)- MN-IBQ	2	28.09	0.92	0.74
40	direct solving	/	/	/	/
40	multi-layer solving ($N = 4$)-Traditional	2	19.64	0.33	2.78
40	multi-layer solving ($N = 4$)- MN-IBQ	2	19.64	0.33	2.34

Figures 10–11 respectively show angle of attack and pitch angle curves calculated by the proposed multi-layer solving method.

From Table 4, conclusions can be obtained as follows:

(1) In engine failure situations, the traditional direct solving method can only converge when the node number N is less than 20, and its positional and velocity accuracies cannot meet the requirements;

(2) The proposed multi-layer solving method has strong robustness against the engine failure situation where the convergent solution cannot be obtained by the traditional direct solving method. That is, for N = 20 and N = 40, the convergent solution cannot be obtained by the direct solving method, but can be rapidly solved by the proposed multi-layer solving method;
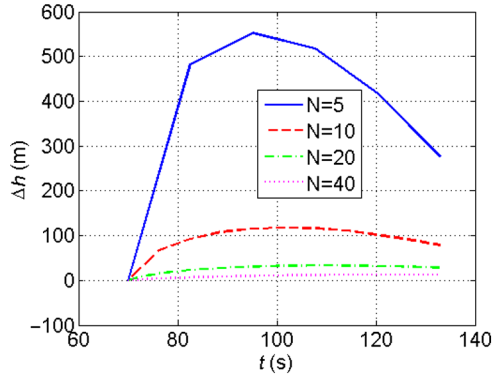
Figure 8. Time-dependent variation of height deviation for engine failure.
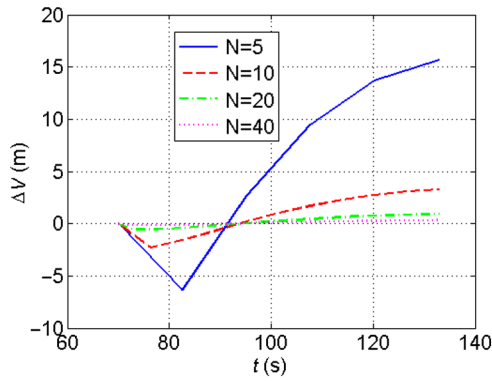

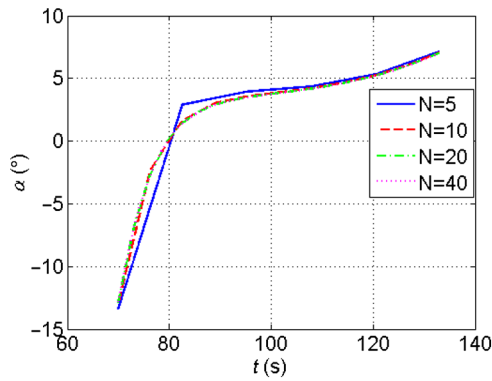Figure 9. Time-dependent variation of velocity deviation for engine failure.

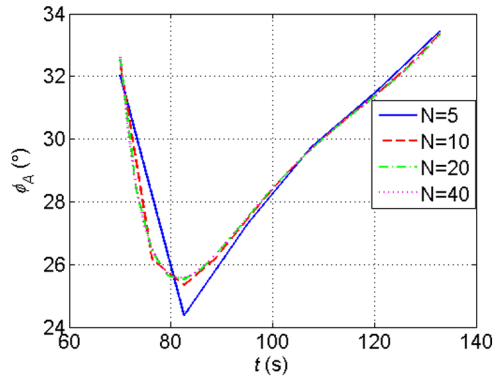Figure 10. Time-dependent variation of angle of attack for engine failure.

Figure 11. Time-dependent variation of pitch angle for engine failure.

(3) For the multi-layer solving method, the positional accuracy and velocity accuracy of optimal ascent trajectory gradually increase with the increase of the number of discrete intervals. N = 40 is enough to obtain the required accuracy $\Delta r \leq 20m$;

(4) Through the combination of the modified Newton method with a relaxation factor and the inverse Broyden quasi-Newton method, the solving rate can be further increased by approximately 15% compared with the traditional Newton method with a relaxation factor. The consuming time of CPU is 2.34 seconds, which can meet the requirement of the online computation speed.

5.0 CONCLUSION

This paper proposes a rapid multi-layer solving method with improved numerical algorithms for solving the optimal endo-atmospheric ascent trajectory problem of a launch vehicle. Numerical simulations show that:

(1) With the same number of discrete intervals, the multi-layer method and traditional method share almost the same solving precision, while the solving rate of the multi-layer method is more than 3 times as fast as that of the traditional method. The proposed multi-layer solving method can be applied to trajectory online generation and closed-loop guidance of launch vehicles at the ascent stage.

(2) In order to further improve the solving efficiency from the perspective of the numerical algorithm, two improved numerical algorithms without and with fewer Jacobian calculations, namely, DF-SANE and MN-IBQ, were studied for solving the finite difference equation.

  i. Although the DF-SANE algorithm theoretically has a higher solving efficiency, it shows poor convergence in solving the complex nonlinear TPBVP. It seems that the failure of DF-SANE is essentially due to the fact that the search direction in DF-SANE is not the descent direction and the non-monotone linear search method has insufficient global convergence.

  ii. Through the MN-IBQ algorithm with fewer Jacobian calculations, the solving rate can be further increased by approximately 15 percent compared with the traditional Newton method with a relaxation factor.

(3) Typical engine failure simulations showed that the proposed multi-layer solving method with the MN-IBQ algorithm had not only significantly higher solving speed but also stronger robustness against the engine failure situation where the convergent solution could not be obtained by the traditional direct solving method. The tolerance limit of thrust loss for the multi-layer solving method increases approximately linearly with the engine failure time.

Declaration of conflicting interests

The author(s) declared no potential conflicts of interest with respect to the research, authorship and/or publication of this article.

Funding

REFERENCES

1. DUKEMAN, G.A. Atmospheric ascent guidance for rocket-powered launch vehicles, AIAA Guidance, Navigation, and Control Conference and Exhibit, AIAA, Reston, VA, 2002.
2. DUKEMAN, G.A. and CALISE, A.J., Enhancements to an atmospheric ascent guidance algorithm, AIAA Guidance, Navigation, and Control Conf. and Exhibit, AIAA Reston, VA, 2003.
3. HANSON, J.M., SHRADER, M.W. and CRUZEN, C.A. Ascent guidance comparisons, *J Astronaut Sci*, 1995, **43**, (3), pp 307–326.
4. GRABLIN, M.H., TELAAR, J. and SCHOTTLE, U.M. Ascent and reentry guidance concept based on NLP-methods, *Acta Astronautica*, 2004, **55**, (3), pp 461–471.
5. ZHANG, D., LIU, L. and WANG, Y. On-line ascent phase trajectory optimal guidance algorithm based on pseudo-spectral method and sensitivity updates, *J Navigation*, 2015, **68**, (6), pp 1056–1074.
6. MAHMOUD, A.M., WANCHUN, C., HAO, Z. and YANG, L. Trajectory optimization for ascent and glide phases using gauss pseudospectral method, *Int J Model Optim*, 2016, **6**, (5), pp 289–295.
7. CALISE, A.J., TANDON, S., YOUNG, D.H. and KIM, S. Further improvements to a hybrid method for launch vehicle ascent trajectory optimization, AIAA Guidance, Navigation, and Control Conf. and Exhibit, AIAA, Reston, VA, 2000.
8. GATH, P.F. and CALISE, A. Optimization of launch vehicle ascent trajectories with path constraints and coast arcs, *J Guid Control Dynam*, 2001, **24**, (2), pp 296–304.
9. LU, P., SUN, H. and TSAI. B. Closed-loop endoatmospheric ascent guidance, *J Guid Control Dynam*, 2003, **26**, (2), pp 283–294.
10. LU, P., GRIFFIN, B.J., DUKEMAN, G.A. and CHAVEZ, F.R. Rapid optimal multiburn ascent planning and guidance, *J Guid Control Dynam*, 2008, **31**, (6), pp 1656–1664.
11. OSCAR, J., MURILLO, J. and LU, P. Fast ascent trajectory optimization for hypersonic air-breathing vehicles, AIAA Guidance, Navigation, and Control Conf. and Exhibit, AIAA, Reston, VA, August 2010
12. CHI, Z., YANG, H., CHEN, S. and LI, J. Homotopy method for optimization of variable-specific-impulse low-thrust trajectories, *Astrophys Space Sci*, 2017, **362**, (11), 216.
13. HUANG, P., WEI, C., GU, Y. and CUI, N. Hybrid optimization approach for rapid endo-atmospheric ascent trajectory planning, *Aircr Eng Aerosp Technol*, 2016, **88**, (4), pp 473–479.

14. SONG, E.J., CHO, S. and ROH, W.R. Analysis of targeting method for closed-loop guidance of a multi-stage space launch vehicle, *Adv Space Res*, 2016, **57**, (7), pp 1494–1507.
15. CRUZ, W.L., MARTINEZ, J.M. and RAYDAN, M. Spectral residual method without gradient information for solving large-scale nonlinear systems of equations *Math Comput*, 2006, **75**, (255), pp 1429–1448.
16. GRIPPO, L., LAMPARIELLO, F. and LUCIDI, S. A nonmonotone line search technique for Newton's method, *SIAM J Numer Anal*, 1986, **23**, pp 707–716.
17. LI, D.H. and FUKUSHIMA, M. A derivative-free line search and global convergence of Broyden-like method for nonlinear equations, *Optim Methods Softw*, 2000, **13**, pp 181–201.
18. KVAALEN, E. A faster broyden method, *Bit Numer Math*, 1991, **31**, (2), pp 369–372.